# Study on the Gel to Crystal Transition of a Novel Sugar-Appended Gelator

**ARTICLE** *in* LANGMUIR · AUGUST 2009

Impact Factor: 4.46 · DOI: 10.1021/la9021382 · Source: PubMed



**3 AUTHORS**, INCLUDING:

Jiaxi Cui
Harvard University
**38** PUBLICATIONS **722** CITATIONS

SEE PROFILE

Langmuir
Article
pubs.acs.org/Langmuir


# Study on the Gel to Crystal Transition of a Novel Sugar-Appended Gelator

Jiaxi Cui, Zhihao Shen,* and Xinhua Wan*

*Beijing National Laboratory for Molecular Sciences, Key Laboratory of Polymer Chemistry and Physics of Ministry of Education, College of Chemistry and Molecular Engineering, Peking University, Beijing 100871, China*

*Received June 15, 2009. Revised Manuscript Received July 15, 2009*

4-(4′-Ethoxyphenyl)phenyl-β-*O*-D-glucoside (**1**) was synthesized. A perfect crystal of **1** was obtained from an acetonitrile solution. In a mixture of water/1,4-dioxane (8/2, v/v), a gel formed at first and then collapsed into a needlelike crystal. The crystal and the gel were characterized by X-ray diffraction, UV−vis absorption, circular dichroism, Fourier transform infrared spectroscopy, and electron microscopy. It was found that the crystal formed from the gel had the same diffraction pattern as that of the single crystal from the acetonitrile solution, suggesting identical molecular packing. In a monoclinic cell containing two molecules, molecules took a "T" arrangement with an antiparallel direction. In contrast, the diffraction pattern of xerogel from water/1,4-dioxane (8/2, v/v) displayed a *d*-spacing ratio of 1:1/2:1/3 (2.39, 1.18, and 0.78 nm), indicating an interdigitated bilayer structure. A molecular packing model from gel to crystal where molecular sheets would insert into each other with a glide movement was suggested. On the basis of the understanding of the deformation mechanism, an additive was introduced to obtain a stable gel.

## Introduction

In the past one or more decades, low molecular mass gelators (LMMGs) have aroused wide attention from both theoretical and practical viewpoints.[1−4] These small organic compounds can efficiently immobilize various solvents through the formation of three-dimensional networks made up of fibrous aggregates.[5−11] To gel a given solvent, elegant molecular design is necessary to keep the balance between crystallization and solubilization of LMMGs.[2] Generally, strong self-complementary and unidirectional noncovalent interactions are needed to drive one-dimensional growth of building blocks.[12] Moreover, some favorable factors that induce the cross-linking of primary aggregates such as fibrils and microcrystals to form networks are also required.[13] However, because such secondary interactions are complex even in a simple system, it is still a rigorous challenge for chemists to synthesize effective LMMGs.

One important yet open question concerning the molecular design of LMMGs is the relationship between the packing of gelator molecules in their bulk crystals and multiple less ordered aggregates in gels.[14] The answer to this question may help not only tune the supramolecular structures of LMMGs in gel by tailoring their intermolecular interactions but also prevent the collapse of the gels formed by LMMGs, which is one of the main disadvantages of this kind of material when compared to polymer gels. Various tools have been used to probe the molecular packing of LMMGs in self-assembled fibrous aggregates, including IR, UV−vis absorption, fluorescence, NMR spectroscopy, and X-ray diffraction and scattering techniques. However, many of these methods supply limited or indirect information about the molecular packing. The main reason is the complexity and hierachical structures of the wet gel.[2] In contrast, single-crystal X-ray crystallography supplies the most accurate and complete information on molecular conformation and packing in the solid phase.[14] However, when such a tool is used to study the molecular packing in a gel, two problems are encountered. First, it is usually difficult to obtain gelator crystals, which are suitable for X-ray diffraction experiments, because these molecules aggregate to form gel fibers or thin needles instead of large crystals. Second, it is very difficult to establish the difference in molecular packing between single crystals and gels because gels and crystals always come from distinctly different conditions. Therefore, few systematic researches on the influence of molecular packing to molecular gelling ability have been reported. For example, an early work by Weiss et al. reported a novel method to discern the packing of gelators within fibers and proved that the gel fiber morphology of cholesterylanthrachion-2-carboxylate differed from the molecular packing of single crystals.[15] In contrast, Menger et al. successfully designed efficient aryl-L-cystine hydrogelators based on the analysis of the crystalline fibrous molecular orientation of the nongelator analogue di(*p*-toluoyl)-L-cystine.[16] Besides, Shinkai et al. analyzed the crystalline structures and gelation behaviors of methyl 4,6-*O*-benzylidene monosaccharides and found that the

*To whom correspondence should be addressed. (Z.S.) Tel: 86-10-62754518. Fax: 86-10-62751708. E-mail: zshen@pku.edu.cn. (X.W.) Tel: 86-10-62754187. Fax: 86-10-62751708. E-mail: xhwan@pku.edu.cn.

(1) Terech, P.; Weiss, R. G. *Chem. Rev.* **1997**, *97*, 3133–3160.
(2) Estroff, L. A.; Hamilton, A. D. *Chem. Rev.* **2004**, *104*, 1201–1218.
(3) van-Bommel, K. J. C.; Friggeri, A.; Shinkai, S. *Angew. Chem., Int. Ed.* **2003**, *42*, 980–999.
(4) van Esch, J. H.; Feringa, B. L. *Angew. Chem., Int. Ed.* **2000**, *39*, 2263–2266.
(5) Becerril, J.; Burguete, M. I.; Escuder, B.; Luis, S. V.; Miravet, J. F.; Querol, M. *Chem. Commun.* **2002**, *2*, 738–739.
(6) Yoza, K.; Ono, Y.; Yoshihara, K.; Akao, T.; Shinmori, H.; Takeuchi, M.; Shinkai, S.; Reinhoudt, D. N. *Chem. Commun.* **1998**, 907–908.
(7) Nolte, R. J. M. *Chem. Commun.* **1997**, 545–546.
(8) Pao, W. J.; Stetzer, M. R.; Heiney, P. A.; Cho, W.-D.; Percec, V. *J. Phys. Chem. B* **2001**, *105*, 2170–2176.
(9) Furman, I.; Weiss, R. G. *Langmuir* **1993**, *9*, 2084–2088.
(10) Jung, J. H.; John, G.; Masuda, M.; Yoshida, K.; Shinkai, S.; Shimizu, T. *Langmuir* **2001**, *17*, 7229–7232.
(11) Zhan, C.; Wang, J.; Yuan, J.; Gong, H.; Liu, Y.; Liu, M. *Langmuir* **2003**, *19*, 9440–9445.
(12) Gronwald, O.; Shinkai, S. *Chem.—Eur. J.* **2001**, *20*, 4328–4334.
(13) Liu, X. Y.; Sawant, P. D.; Tan, W. B.; Noor, I. B. M.; Pramesti, C.; Chen, B. H. *J. Am. Chem. Soc.* **2002**, *124*, 15055–15063.
(14) Brizard, A.; Oda, R.; Huc, I. *Topics in Current Chemistry*; Springer-Verlag: New York, 2005; Vol. *256*, pp 167−218.
(15) Ostuni, E.; Kamaras, P.; Weiss, R. G. *Angew. Chem., Int. Ed.* **1996**, *35*, 1324–1326.
(16) Menger, F. M.; Caran, K. L. *J. Am. Chem. Soc.* **2000**, *122*, 11679–11691.

**Table 1. Crystallographic Data of 1**

| | | | | |
|---|---|---|---|---|
| formula sum | $C_{20}H_{24}O_7$ | unit cell dimensions | $a$ = 7.5581(2) Å | $b$ = 7.8679(2) Å |
| formula weight | 376.39 | | $c$ = 16.1177(4) Å | $\beta$ = 103.34(0) ° |
| crystal system | monoclinic | cell volume | 932.60(4) Å$^3$ | |
| space group | *P* 1 21 1 (no. 4) | density, calculated | 1.340 g/cm$^3$ | |

molecules that formed an one-dimensional hydrogen-bonding array in a single crystal were good gelators.[12] Both works investigated gelators by analyzing crystal data with an interest in the driving force of formation. In contrast, no study has been reported yet on the deformation of gels, which is very important to prepare a stable gel system.

Herein, we report the hierarchical structures and their transitions of a new sugar-based gelator, 4-(4′-ethoxyphenyl)phenyl-*β*-*O*-D-glucoside (**1**), in the mixture of water and 1,4-dioxane. Compound **1** gels a number of solvents such as acetone, *n*-butanol, and 1,2-dichloroethane at concentrations as low as 5 mg/mL . In the mixed solvent of water/1,4-dioxane, the gel−crystal transition could be tuned by changing the composition of the solvent, which provided a suitable window to approach its molecular packing in fibrous aggregate and the structural evaluation that caused the gel to collapse. A combinatory analysis of the X-ray data of single crystals, xerogels, and fiber crystals, UV−vis spectra, circular dichroism (CD) spectra, and Fourier transform infrared (FT-IR) spectra of crystals and oxerogels demonstrated that **1** formed an interdigitated bilayer structure in the gel state and the layers would insert into each other to drive the gel to evolve into a fibrous crystal where **1** was packed with herringbone arrays that were characterized by nearest-neighbor edge-to-face interactions.

## Results

**Single Crystal Structure.** The novel gelator **1** was synthesized with a similar method as in ref 17. It consisted of a glycosyl head, a biphenyl core, and an ethoxy tail. The $^1$H NMR spectrum of **1** exhibited only one doublet with $J$ = 6.6 Hz for the anomeric proton, indicating a 100% *β*-glucosidic linkage.[18] The single crystal of **1** was obtained from acetonitrile. Detailed crystallographic data are summarized in Table 1, and the key bond distances and angles are listed in Table S1 of the Supporting Information. Detailed molecular geometries were retrieved from the cif files. X-ray crystallography indicated that it was monoclinic with $a$ = 7.56 Å, $b$ = 7.87 Å, $c$ = 16.12 Å, and $\gamma$ = 103.34° (Table 1 and Figure 1). In a unit cell (Figure 1a), two molecules were stacked in a "T" arrangement (edge-to-face) with an antiparallel direction, suggesting a chiral pinwheel structure.[19] An intermolecular hydrogen bonding (H-bonding) formed between the O7 of one molecule and the hydrogen atom of O6 in the glycosyl of the neighboring molecule. The top and side views (Figure 1b,c) showed that each molecule contributed eight intermolecular H-bonding, which formed a two-dimensional hydrogen-bonding network (plane of o′ob). Among them, four (a−d in Figure 1a) formed between the molecules in the o→b direction (Figure 1b), and the other four (e−h) formed in the o→o′ direction. In addition, biphenyl groups positioned in the core of this two-dimensional network showed a poor $\pi-\pi$ interaction (it would be further proved below by UV−vis spectra) due to their long distances (7.56 or 7.87 Å). In the third direction (o→a), **1** formed a herringbone array with aromatic CHs pointing toward the face of the biphenyl moiety of the adjacent molecules. The short distance between the hydrogen atom and the centers of the

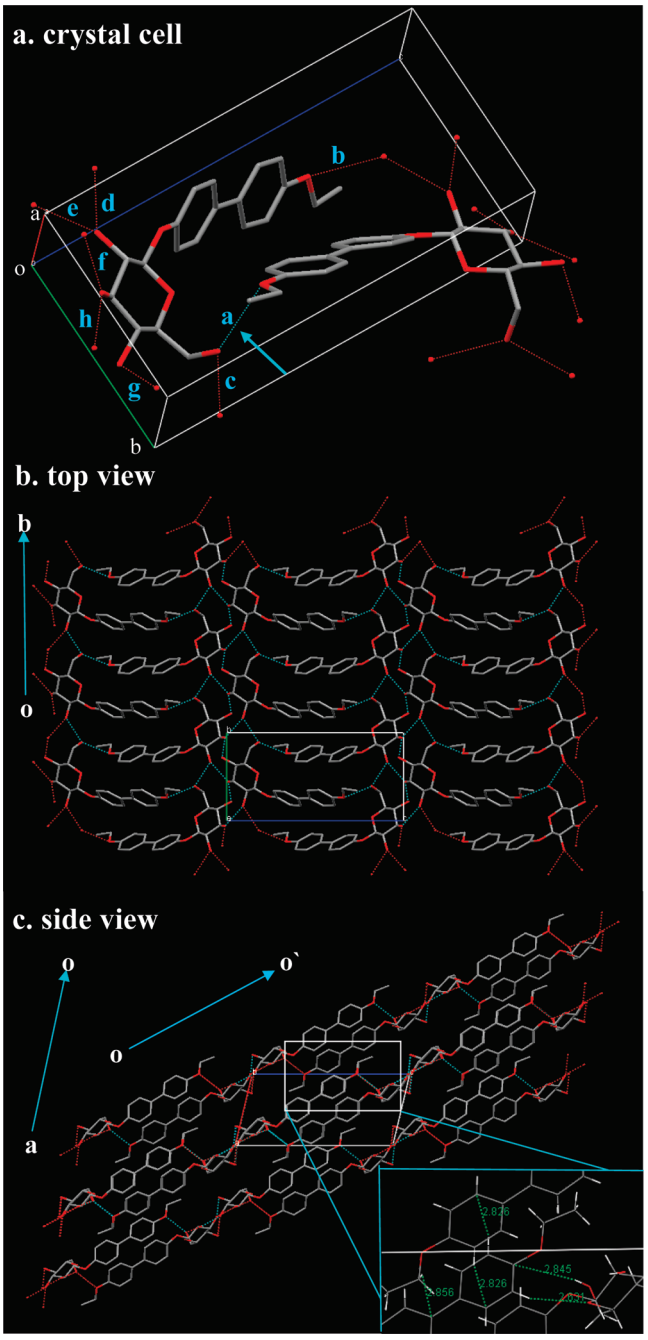


**Figure 1.** Molecular packing of **1** in single crystal from acetonitrile: (a) monoclinic cell, H-bonding is shown by the arrowhead; (b) top view, dotted line represents H-bonding; and (c) side view, the inset shows the short contact that is summarized by van der Waals radii.

aromatic rings (283 pm, the hydrogen atoms at C15 and C18, as shown in the insert of Figure 1c) were shorter than the sum of the van der Waals radii of the relevant atoms, indicating a edge-to-face (CH/$\pi$) aromatic interaction.[20,21] Additionally, another three

(17) Muller, H.; Tschierske, C. *J. Chem. Soc., Chem. Commun.* **1995**, 645–646.
(18) Shimizu, T.; Masuda, M. *J. Am. Chem. Soc.* **1997**, *119*, 2812–2818.
(19) Whitten, D. G.; Chen, L.; Geiger, H. C.; Perlstein, J.; Song, X. *J. Phys. Chem. B* **1998**, *102*, 10098–10111.
(20) Wolfgang, B.; Fritz, V.; Martin, N.; Heike, H. *Chem.—Eur. J.* **1999**, *5*, 345–355.
(21) Nishio, M. *CrystEngComm* **2004**, *6*, 130–158.

**Table 2. Gelation Behavior of 1 in Various Solvents at 25 °C[a]**

| solvent | hexane | $CCl_4$ | toluene | $CHCl_3$ | $CH_2ClCH_2Cl$ | ethyl acetate | acetonitrile |
|---|---|---|---|---|---|---|---|
| | I | I | I | Gp | G | P | P |
| solvent | 1,4-dioxane | THF | acetone | n-butanol | ethanol | DMF | $H_2O$ |
| | S | S | G | G | P | S | P |

[a] Concentrations: 0.5 mg/mL in water and 5 mg/mL in other solvents. G, gel; S, solubilization; I, insolubilization; P, precipitation; and Gp, partial gel.

**Table 3. Gelation Behavior of 1 in Water/1,4-Dioxane Mixed Solvent at a Concentration of 5 mg/mL [a]**

| water/1,4-dioxane (v/v) | 10/0 | 9.5/0.5−8/2 | 7.5/2.5−6.5/3.5 | 6/4−0/10 |
|---|---|---|---|---|
| gelability | P | G | P | S |

[a] P, precipitation; G, gel; S, solubilization; and temperature, 25 °C.

**Table 4. Gelation Behavior of 1 in Water/1,4-Dioxane (8/2, v/v) at Different Concentrations[a]**

| concentration (mg/mL) | 0−0.01 | 0.01−0.05 | 0.05−3 | >3 |
|---|---|---|---|---|
| gelability | S | Gp | G | $G_I$ |

[a] G, gel; S, solubilization; Gp, partial gel; $G_I$, gel with solids; temperature, 25 °C.

**Table 5. Gel Stability of 1 at Various Temperatures[a]**

| temperature (°C) | 2 | 10 | 25 | 50 |
|---|---|---|---|---|
| time (h)[b] | >240 | 160 | 24 | 2 |

[a] Concentration, 5 mg/mL ; solvent, water/dioxane (8/2, v/v); and temperature, 25 °C. [b] The time that the gel does not collapse.

CH/$\pi$ interactions formed between the hydrogen atoms at ethoxyl or glycosyl and the aromatic (286 pm for the hydrogen at C19, 263 pm for the hydrogen at C17, and 285 pm for hydrogen at O6, as shown in the insert of Figure 1c). Although this interaction was weaker than the hydrogen-bonding interaction, it might play an important role when the molecules grow up as a bundle.[22]

**Gelation Experiments.** Fourteen solvents were employed to evaluate the gelling ability of **1**. The results are summarized in Table 2. It was evident that **1** dissolved in the three polar solvents selected, dimethyl formamide (DMF), tetrahydrofuran (THF), and 1,4-dioxane, but did not dissolve in the three apolar solvents, tetrachloromethane, cyclohexane, and toluene. In water, ethanol, ethyl acetate, and acetonitrile, crystals precipitated from the hot solution, whereas in acetone, 1,2-dichloroethane, *n*-butanol, and chloroform, stable and partial gels were generated, respectively. Interestingly, in the mixture of water/1,4-dioxane, a gel formed at first but collapsed into thin crystals after a certain time, depending on the composition of the solvent, temperature, and the concentration of **1** (Tables 3−5). For example, 5 mg/mL of **1** in water/1,4-dioxane (8/2, v/v) exhibited a gel state for 24 h at 25 °C but no more than 2 h at 50 °C. The tunable gel-to-crystal transition should help elucidate the molecular packing of **1** in its fibrous aggregates. On the other hand, it supplied a suitable window to probe the collapse mechanism of the gel.

**TEM and WAXD.** Figure 2 shows the self-assembled morphologies of **1** in xerogel and in a collapsed crystalline state. The xerogel of **1** showed a three-dimensional network made up of helical ribbons with a width of tens of nanometers. When the gel collapsed, slender flat crystals were observed. According to the theories of self-assembled helical ribbons,[23] the helicity of ribbons came from the twist in the molecular level due to molecular elasticity.[24] Wide-angle X-ray diffraction (WAXD) was used to probe the molecular packing of **1** in either the xerogel or the bulk crystal. As shown in Figure 3, the crystal from the collapsed gel had the same diffraction pattern as that of the single crystal from acetonitrile, suggesting the same molecular packing. In contrast, the xerogel displayed a series of diffractions in the low-angle region and there were three reflection peaks centered at $2\theta = 3.69$, 7.48, and 11.34°, respectively (Figure 3c). The ratio of the corresponding *d*-spacings (2.39, 1.18, and 0.78 nm) was 1:1/2:1/3, indicating a lamellar structure. The *d*-spacing of 2.39 nm corresponding to the strongest diffraction was smaller than twice but larger than the upmost length of **1** (1.65 nm, estimated from C20 to O3, Chart 1). It might be concluded that **1** formed an interdigitated bilayer structure with a thickness of 2.39 nm in water/1,4-dioxane (8/2, v/v).

**FT-IR Spectra.** Figure 4 shows the infrared spectra of the xerogel and crystal of **1**. The spectrum of the xerogel exhibited one band centered at 821 $cm^{-1}$ with a slight shoulder band at 810 $cm^{-1}$, while that of the crystal showed two bands centered at 825 and 810 $cm^{-1}$, respectively. These bands represented the out-of-plane bending vibration of C−H in biphenyl. Compound **1** had different substituted groups at the two-terminal of the biphenyl core, which would influence the vibration frequency of C−H in the aromatic core due to an inductive effect.[25] However, the difference between ethoxyl and glycosyl in the inductive effect was small due to their electronic donor property; therefore, only a slight shoulder band was observed, as that in the case of its analogous compound.[26] In contrast, the band centered at 821 $cm^{-1}$ in the xerogel blue shifted to 825 $cm^{-1}$ in the crystal, suggesting that some interaction influences the vibration of the out-of-plane C−H.[27] In the discussion of crystallographic data, the appearance of CH/$\pi$ aromatic interaction has been suggested. Herein, the energy change of the blue shift of 4 $cm^{-1}$ was coincident with CH/$\pi$ complex formation.[27] Therefore, it was supposed that the observable splitting bands probably contributed from the CH/$\pi$ interaction in the crystal state. Furthermore, the bands of 3100−3500 $cm^{-1}$ that represented H−O stretching vibration were different for the xerogel and crystal. The spectrum of the crystal exhibited three bands centered at 3338, 3406, and 3471 $cm^{-1}$, respectively, while that of the xerogel only displayed one band centered at 3376 $cm^{-1}$. From the crystallography data (Table S1), it was found that the bond lengths of H and O were different, 0.88 (2) Å for O2−H2 and O4−H4, 0.84 (2) Å for O6−H6, and 0.81 (3) Å for O3−H3. The various bond lengths were attributed to the H-bonding interaction, for example, g for O2−H2, d and e for O4−H4, a and c for O6−H6, and f and h for O3−H3 (Figure 1a). The vibration frequency was the function of bond strength. Therefore, it can be proposed that the absorption of 3338 $cm^{-1}$ came from O2−H2 and O4−H4, that of 3406 $cm^{-1}$ from O6−H6, and that of 3471 $cm^{-1}$ from O3−H3. The spectrum of xerogel only displayed one broadband of 3376 $cm^{-1}$. The appearance of the broadband should be attributed to the merger of various stretching vibrations in the xerogel state that were weaker than that of 3338 $cm^{-1}$ but stronger than that of 3406 $cm^{-1}$. In addition, the change in the area of 1000−1150 $cm^{-1}$

(22) Grossel, M. C.; Cheetham, A. K.; Hope, D. A. O.; Weston, S. C. *J. Org. Chem.* **1993**, *58*, 6654–6661.
(23) Selinger, J. V.; Spector, M. S.; Schnur, J. M. *J. Phys. Chem. B* **2001**, *105*, 7157–7169.
(24) Nandi, N.; Bagchi, B. *J. Am. Chem. Soc.* **1996**, *118*, 11208–11216.
(25) Leonard, N. J.; Owens, F. H. *J. Am. Chem. Soc.* **1958**, *80*, 6039–6045.
(26) Cui, J.; Zheng, J.; Qiao, W.; Wan, X. *J. Colloid Interface Sci.* **2008**, *326*, 267–274.
(27) Sundararajan, K.; Sankaran, K.; Viswanathan, K. S.; Kulkarni, A. D.; Gadre, S. R. *J. Phys. Chem. A* **2002**, *106*, 1504–1510.

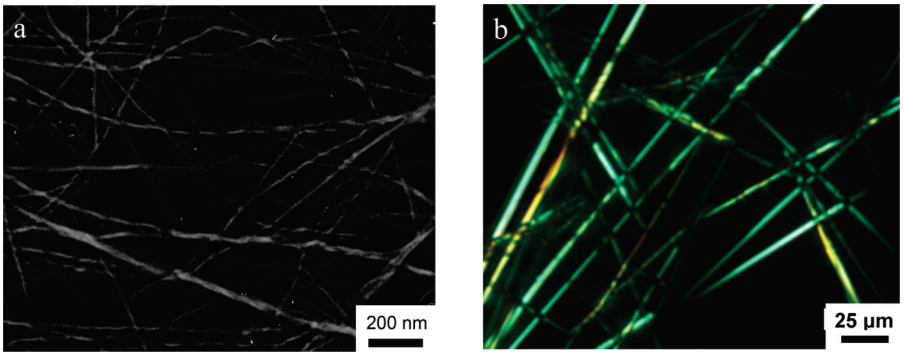


**Figure 2.** TEM (a) and POM (b) images of the gel of **1** in water/1,4-dioxane (8/2, v/v; 5 wt ).

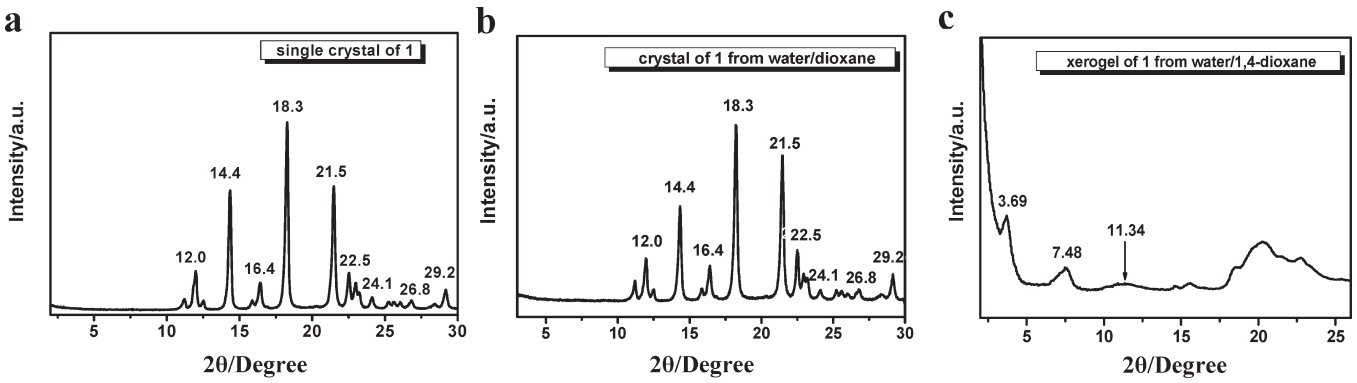


**Figure 3.** XRD of (a) a single crystal of **1** from acetonitrile (2 mg/mL ), (b) a crystal of **1** from water/1,4-dioxane (8/2, v/v, 5 mg/mL ), and (c) a xerogel of **1** from water/1,4-dioxane (8/2, v/v, 5 mg/mL ).

**Chart 1. 4-(4′-Ethoxyphenyl)phenyl-*β*-*O*-D-glucoside**

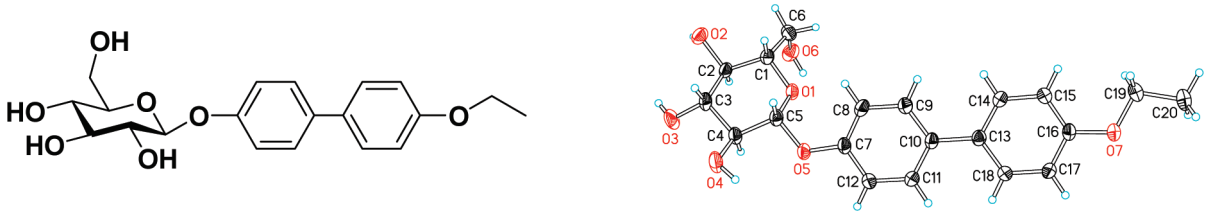


assigned to the stretching vibration of the glycosyl ring illustrated different conformations in various states.

**UV−vis Spectra.** As shown in Figure 5, **1** in 1,4-dioxane, a good solvent, exhibited a band at 266 nm, which was assigned to $^1L_a$ of biphenyl.[19,28] As compared with that in 1,4-dioxane, the absorption band of **1** in the gel of water/1,4-dioxane blue shifted 8 nm, and one shoulder band at 283 nm (a low-lying $^1L_b$ state), which was covered by the strong absorption of $^1L_a$ in solution phase, appeared.[29] The KBr tablet containing a freeze-dried xerogel showed a similar blue shift. The blue shift illustrated not only a strong $\pi-\pi$ stacking interaction in the gel but also an "H" aggregated arrangement.[30−32] In contrast, the crystal showed a broadband centered at 268 nm, suggesting weak $\pi-\pi$ interaction. It can be ascribed to the long distances between biphenyl rings (0.756 and 0.787 nm) in the crystal phase. Whereas the slight red shift from 266 to 268 nm might be due to a CH/$\pi$ interaction. Simultaneously, the shoulder band at 283 nm with a long tail to the range of 300−350 nm became more observable maybe due to the better conjugate action of the biphenyl core in the solid state.[29,30]

**CD Spectra.** Figure 6 shows the CD spectra of **1** under various conditions. In the solution state, **1** exhibited no discernible Cotton effect, indicating that the chiral sugar head was relatively far from the biphenyl chromophore and that the chiral aggregate was absent. The CD spectrum of the KBr tablet of the crystal displayed two conservative Cotton effects. The spectrum intersected the abscissa at 268 nm, which corresponded to the wavelength of maximum absorption. Such exciton-coupling CD bands can be ascribed to the chiral "pinwheel" in herringbone arrays.[19] In contrast, **1** in a gel showed two intensive negative CD bands centered at 244 and 262 nm, respectively, and a shoulder band at 283 nm. When the solvents were removed, the negative band at 244 nm turned out to be a positive one and the band at 262 nm shifted to 267 nm. The two bands intersected the abscissa at 253 nm, the position of absorption maximum. Furthermore, the negative shoulder band shifted to 298 nm, and a positive CD

(28) Geiger, H. C.; Perlstein, J.; Lachicotte, R. J.; Wyrozebski, K.; Whitten, D. G. *Langmuir* **1999**, *15*, 5606–5616.
(29) Dutta, A. K.; Misra, T. N.; Pal, A. J. *J. Phys. Chem.* **1994**, *98*, 12844–12848.
(30) Momicchioli, F.; Bruni, M. C.; Baraldi, I. *J. Phys. Chem.* **1972**, *76*, 3983–3990.
(31) Nakahara, H.; Fukuda, K.; Moebius, D.; Kuhn, H. *J. Phys. Chem.* **1986**, *90*, 6144–6148.
(32) Kemnitz, K.; Tamai, N.; Yamazaki, I.; Nakashima, N.; Yoshihara, K. *J. Phys. Chem.* **1986**, *90*, 5094–5101.

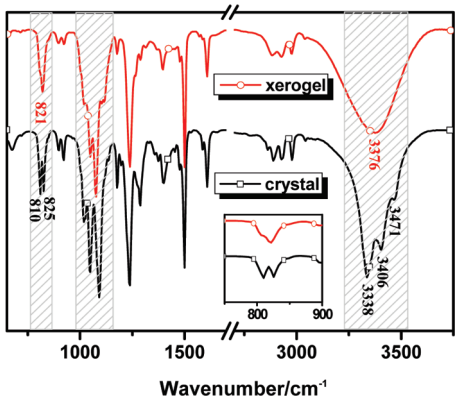


**Figure 4.** FT-IR spectra of the xerogel of **1** from water/1,4-dioxane ((8/2, v/v, 5 mg/mL, ○) and the crystal from acetonitrile (□) at 25 °C; the inset is the amplificatory part.

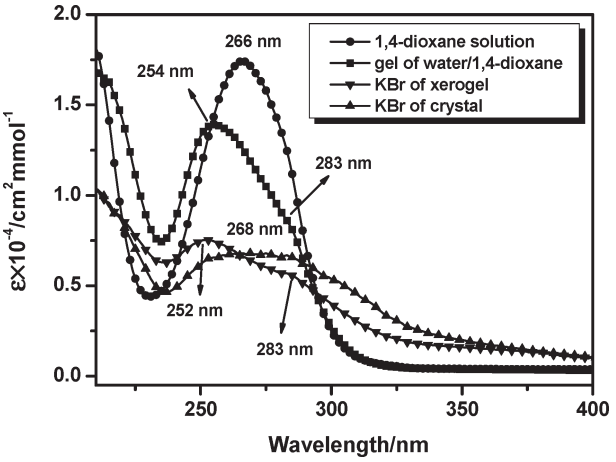


**Figure 5.** UV−vis spectra of **1** in 1,4-dioxane (●; light path length, 0.1 mm; 5 mg/mL ), water/1,4-dioxane (8/2, v/v, ■; light path length, 0.2 mm; 5 mg/mL ), KBr tablet containing the xerogel from water/1,4-dioxane (8/2, v/v, ▼; 80 mg of mixture; 0.1 wt % ), and KBr tablet containing the crystal from acetonitrile (▲; 80 mg of mixture; 0.1 wt % ) at 25 °C.

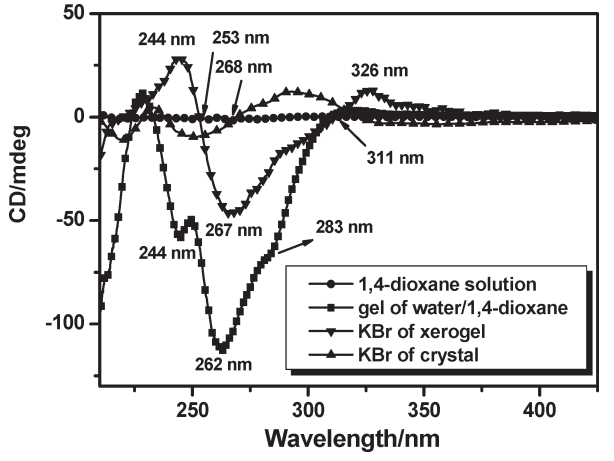


**Figure 6.** CD spectra of **1** in 1,4-dioxane (●; light path length, 0.1 mm; 5 mg/mL ), water/1,4-dioxane (8/2, v/v, ■; light path length, 0.1 mm; 5 mg/mL ), a KBr tablet containing the xerogel from water/1,4-dioxane (8/2, v/v, ▼; 80 mg of mixture; 0.1 wt % ), and a KBr tablet containing the crystal from acetonitrile (▲; 80 mg of mixture; 0.1 wt % ) at 25 °C.

band at 326 nm appeared. The two bands intersected the abscissa at 311 nm. The appearance of the exciton-coupling peaks might be because of the approach of the molecules after the removal of solvents.

## Discussion

As compared to its analogous compound, 4-(4′-butoxyphenyl)phenyl-*β*-*O*-D-glucoside (C4BG),[26] **1** exhibited poorer gelling ability. C4BG acted as an excellent gelator of water, acetonitrile, ethyl acetate, chloroform, toluene, *n*-butanol, and the mixture of water and 1,4-dioxane. Increasing the content of 1,4-dioxane in water caused a gradual transformation from planar to twisted ribbons and then tubes. In a sharp contrast, **1** only gelled acetone, *n*-butanol, and 1,2-dichloroethane and partially gelled chloroform. In the mixture of water and 1,4-dioxane, the gels formed were unstable. Similar to C4BG, **1** also had a amphiphilic structure with a hydrophilic glycosyl head, a hydrophobic biphenyl core, and an ethoxy tail, suggesting the same driving forces for the gelation.[26] In water, the sugar head of **1** is soluble, and a hydrophobic interaction and $\pi-\pi$ stacking between aromatic rings supplied the driving forces for the molecules to aggregate, whereas in a less polar solvent, the main driving force originated from the H-bonding among the glycosyl head of gelator.

On the basis of the results above, it can be concluded that **1** formed helical ribbons with an interdigitated bilayer structure in the gel of water/1,4-dioxane (8/2, v/v) where an intralayer $\pi-\pi$ interaction played an important role as that of C4BG.[25] This structure evolved into a tight, "T"-oriented packing with the length of the interdigitated dimer decreasing from 2.39 to 1.93 nm (in the o→o′ direction in Figure 1c) in the crystal. A molecular packing model was suggested to describe the evolution of molecular packing from gel to crystal, as shown in Figure 7.

In the gel phase, **1** formed bilayers with an overlap of ethoxyl (Figure 7a). Because only the alkyl part was interdigitated, the distances between biphenyl rings (r in Figure 7a) were short and therefore exhibited strong intralayer $\pi-\pi$ interactions. The biphenyl planes were parallel in one interdigitated molecular sheet (e.g., solid one in Figure 7) but displayed an inclined angle ($\theta$) to that of another molecular sheet (e.g., hollow one in Figure 7). Because of the damaging effect of water, the intermolecular H-bonding of the sugar head was weak. Meanwhile, the intermolecular edge-to-face aromatic interaction was absent. The $\pi-\pi$ interaction between biphenyls, a unidirectional interaction to enforce one-dimensional self-assembly, increased to be dominant in molecular packing. It was a loose packing where molecules were stacked at a slight angle with respect to their neighbors due to chiral molecular elasticity, resulting in a helical morphology.

Fibrils in the gel state tended to align together driven by surface tension.[26,33] Simultaneously, the interaction between overlapping ethoxy tails was not strong enough to maintain the bilayer structure under the pressure of neighboring molecular sheets due to the surface tension, and then, the molecular sheet glided into each other, and the tails inserted into the interspace of biphenyls (Figure 7b). With the gliding of ethoxyl, the distance r increased, resulting in the weakening of the $\pi-\pi$ interaction. The H-bonding between glycosyls formed in adjacent molecular bilayers. Such H-bonding promoted the fibers to aggregate along the normal direction of the molecular sheet. No H-bonding like a and b formed, and it was an unstable state.

When the ethoxyls were inserted into the position where H-bonding between ethoxyl and glycosyl formed, intermolecular

(33) Boettcher, C.; Schade, B.; Fuhrhop, J. H. *Langmuir* **2001**, *17*, 873–877.

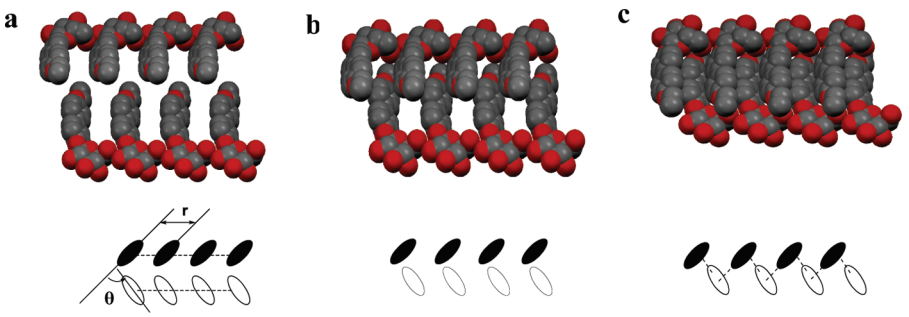


**Figure 7.** Molecular packing model of **1** from gel to crystal.

edge-to-face aromatic interaction appeared (Figure 7c). Here, a twist of the molecular sheet and the $\pi-\pi$ interaction between biphenyls disappeared with the decrease of surface tension. Because fibrils formed first, a lamellar crystal instead of a tetragonal crystal appeared in water/1,4-dioxane.

Consequently, on the basis of the investigation of the evolutionary process of **1** from gel to crystal, a mechanism about molecular packing transformation was suggested as follows: Driven by surface tension, fibrils aggregated together with a glide movement at a molecular level, resulting in the collapse of the three-dimensional network of the gel phase. The key to increase the stability of the gel phase was to prevent the glide movement. Compound **1** had an ethoxy tail, which was too short to form a stable bilayer with overlapping alkoxyl. Increasing the length of the alkoxy tail would enhance the stability of the gel phase, as in the case of C4BG, which had a butoxy tail. On the other hand, the driving force of the glide movement could be attributed to the surface tension between solvent and gelator molecules.[26,33] A subtle change of solution condition would influence the stability of the gel state, as shown in Table 2. Furthermore, gelation is a kinetically controlled process, and a stable gel could be obtained via modulation of the growth of fibers.[34] On the basis of the idea of branching creation by adding a polymer, an interconnection self-organized nanofiber networks from separate needlelike crystals of L-DHL (lanosta-8,24-dien-3-$\beta$-ol:24,25-dihydrolanosterol/56:44) has been achieved by Liu et al.[13] The branching prevented the fiber from aggregating together, which was thought to cause the collapse of the gel. Within the framework of such a concept, polymeric additives would cover the surface of fiber to prevent fibrils from further aggregating to form needlelike crystals. Here, poly(2-hydroxyethyl methacrylate) (PHEMA, MD $\approx$ 50), which contains multihydroxyl, was selected as an additive. A varying amount of PHEMA was added (0.1−2 mg/mL). It was found that once 0.5 mg/mL PHEMA was added [5 mg/mL of **1** in water/1,4-dioxane (8/2, v/v) at 25 °C], a stable gel was achieved, and the gel did not collapse even at 50 °C for more than a week. Although PHEMA used here was soluble in the mixture solvent, it has a hydrophobic main chain. During the formation of the network consisting of the fibrils of **1**, it was supposed that PHEMA took part in the growth of **1** into the network due to its amphiphilic structure. Once the polymer absorbed at the surface of the fibrils, it would not only decrease the surface tension but also prevent fibrils to aggregate further due to the branching effect.[13]

## Conclusion

The gelling behavior of a novel gelator **1** was reported. In its acetonitrile solution, a perfect crystal of **1** was obtained, which supplied complete information about molecular packing. The XRD pattern of the crystal from the collapsed gel of water/1,4-dioxane (8/2, v/v) indicated the same crystal structure. Because **1** formed interdigitated bilayer structure before the gel collapsed into the crystal, a model with single molecular sheets inserting into each other was suggested. In the model, a $\pi-\pi$ stacking interaction weakened, and an intermolecular CH/$\pi$ interaction enhanced with the gliding of molecular sheets. From gel to crystal, molecular packing had an obvious change, illustrating that molecular packing imposed a great impact on the molecular gelling ability. Furthermore, the gel phase of **1** could be stabilized by the addition of PHEMA.

## Experimental Section

**General Methods.** $^1$H NMR and $^{13}$C NMR spectra were recorded on a Bruker ARX400. The chemical shifts ($\delta$) were reported in ppm relative to tetramethylsilane. Elemental analysis was run on a GmbH Vario EL instrument, and the mass spectrum was recorded on a Bruker Inc. BIFLEX III. Optical rotations were measured with a JASCO model P-1030 digital polarimeter using a water-jacketed 100 mm cell. Infrared spectra of the freeze-dried xerogel and single crystal were recorded with micrographic method on a Magna-IR 750 FT-IR spectrometer.

**Gelation Experiments.** In a typical gelation experiment, 5 mg of **1** and 1 mL of solvent were put in a sample vial, and then, the sample vial was tightly sealed with a screw cap. The mixture was dealt with ultrasonically and then heated until all of the solid material had dissolved. The solution was set aside and allowed to cool in air. If the solution did not gel, the bottle was put in a refrigerator at 0−2 °C for 10 min and then placed in air for 1 h. If the solid aggregate mass was stable to inversion, it was believed to be gelled. A PolyScience programmable temperature controller was used for controlling the temperature from 4 to 50 °C.

**Microscopic Observations.** For transmission electron microscopy (TEM), a piece of the gel was put onto the carbon-coated copper grid (400 mesh) and removed after 1 min, leaving some small patches of the gel on the grid. Then, it was dried for 1 h in vacuum. The specimen was examined with a JEM-100CX instrument operated at 120 kV. Images were recorded on negative films. A Leica DML polarized optical microscope (POM) was used for taking the POM images.

**X-ray Crystallography Study.** Crystallographic data for single crystals of **1** were collected at 293 K on a Nonius Kappa CCD diffractometer with a 2.0 kW sealed tube source using graphite monochromated Mo K$\alpha$ radiation of $\lambda$ = 0.71073 Å ("Collect" data collection software; Nonius B.V.: Delft, The Netherlands, 1998). Empirical absorption corrections were applied using the Sortav program ("HKL2000" and "maXus" softwares; University of Glasgow, Scotland, United Kingdom; Nonius B.V.: Delft, The Netherlands and MacScience Co. Ltd.: Yokohama, Japan, 2000). The structures were solved by the direct method and refined by the full-matrix least-squares method on $F^2$ with anisotropic thermal parameters for all nonhydrogen

(34) Liu, X. Y. *Topics in Current Chemistry*; Springer-Verlag: New York, 2005; Vol. *256*, pp 1−37.

atoms, using the SHELX program.[35] Hydrogen atoms attached to carbons were added to calculated positions. Hydrogen atoms of the lattice water were not included. Crystallographic data are given in Table 1, and selected bond distances are in Table S1.

**Powder X-ray Diffractograms.** The X-ray diffraction (XRD) of a freeze-dried sample was measured with a Philips X'Pert Pro diffractometer with a 3 kW ceramic tube as the X-ray source (Cu Kα radiation) and an X'celerator detector. The typical exposure time was 30 min with a 150 mm camera length.

**CD and UV−vis Measurements.** (a) Gel sample: The gelator and solvents were heated to be clear and then injected into the cell with a hot glass sucker. The cell was cooled in air, and then, the solution gelled. (b) Solid sample: 1 mg of dried sample in 1 g of KBr was ground into powder, and 80 mg of mixture was pressed to be a tablet. Eighty milligrams of pure KBr tablet was selected as a reference. UV−vis absorption spectra were obtained with a Varian Cary 1E UV−vis spectrometer with a PolyScience programmable temperature controller for temperatures from 0 to 80 °C, and CD spectra were recorded using a JASCO J-810 spectrometer. The path length of the quartz cell was 0.1 mm in CD measurement and 1 mm in UV−vis measurement.

(35) (a) Sheldrick, G. M. *SHELXTL*, Version 5.1; Bruker Analytical X-ray Instruments Inc.: Madison, WI, **1998**. (b) Sheldrick, G. M. *SHELX-97*, PC Version; University of Göttingen: Germany, **1997**.

**Acknowledgment.** We thank the financial support of the National Natural Science Foundation of China through the General Program (No. 20674001), the Key Program (No. 20834001), the National Distinguished Young Scholars Project (No. 20325415), and the China Postdoctoral Science Foundation (No. 20080440249).

**Supporting Information Available:** $^{1}H$ and $^{13}C$ NMR, mass, elementary analysis results, and specific optical rotation of **1**; bond lengths of **1** in the crystal state. This material is available free of charge via the Internet at http://pubs.acs.org.